nzsee
NEW ZEALAND SOCIETY FOR EARTHQUAKE ENGINEERING

Site-specific seismic hazard evaluation of critical bridge infrastructure in Cebu, Philippines

F.J.T. Bernales, P.A.Y. Selda, R.D. Quebral & R.A.C. Luna
AMH Philippines, Inc., Quezon City, Philippines.

ABSTRACT

Inter-island bridges in active tectonic regions are exposed considerably to elevated seismic risks. Evaluation of the seismic hazard is a primary step in assessing this risk. This paper describes the seismic hazard evaluation of a critical bridge infrastructure in Cebu, Philippines, capitalizing on the knowledge gained from geological investigation efforts as well as project-specific structural information. Existing seismic hazard models were improved through a more refined characterization of seismic sources, site conditions, and intensity measures. Deterministic and probabilistic approaches were compared to provide better insights on the seismic hazard for a reference rock condition—defined as the average shear wave velocity from the 'refusal' layer. From a suite of scaled motions that are spectrum-compatible at the reference rock condition, nonlinear site response analysis was performed for several locations along the bridge alignment to account for spatial and aleatory variability in the site terms. A simple smoothing approach was done to develop the design response spectra at two hazard levels intended to evaluate two different performance objectives. Finally, two different suites of ground motion time histories were modified and matched to the target response spectra using a time-domain response spectrum matching procedure to generate input motions for dynamic analysis of the bridge. This strategy allowed multi-support excitation to account for the incoherence of seismic waves.

1 INTRODUCTION

As an emerging market, the Philippines has been pushing to expand its infrastructure portfolio to sustain economic growth projections. A key component in this portfolio is the construction of inter-island links or bridges to connect several island groups of the Philippine archipelago to major economic hubs. As of 2019, a total of 16 proposed short and long-span bridge projects are on the slate in this infrastructure expansion program (Unite, 2019). Although the potential economic benefits are clear, these inter-island bridges—which can reach up to 20 to 30-km long—pose various design challenges and risks from an engineering perspective due to their vast exposure to natural hazards akin to an active tectonic region like the Philippines.

One of these inter-island links is the proposed critical bridge infrastructure in Cebu, Philippines. In developing the required ground motions for structural analysis and design, local code provisions require a site-specific seismic hazard evaluation, in addition to a general procedure, for very important bridges. This paper details the procedures adopted in the seismic hazard evaluation—site characterization, seismic source modeling, seismic hazard calculation, site response analysis and uncertainty quantification, as well as time history development—consistent with the appropriate level of performance pursuant to the Load and Resistance Factor Design (LRFD) Bridge Seismic Design Specifications (DPWH, 2013; DPWH, 2019).

2 SITE CHARACTERIZATION

Site conditions affect the characteristics of ground motions at a specific location due to the complex interaction of seismic waves with local (to regional) geology and morphology. As such, the seismic hazard evaluation effort depends heavily on the geological and/or geotechnical investigation (GI) program to gain insights into the type and behavior (e.g. stiffness and strength) of materials present at the site. The GI program for the bridge consisted of two cone penetrometer tests (CPT) as well as 19 borehole drilling, standard penetration testing (SPT), and sampling (GPI, 2022). Three of the 19 boreholes—with two located offshore—also had seismic velocity readings measured using the P-S suspension logging method.

Figure 1(a) and (c) present the idealized lithological profiles or stratification for the two offshore locations located 13.31 m and 4.31 m below sea level, respectively. As expected for an offshore site, the borehole data showed the presence of compressible soils which are generally fine-grained soils with SPT N-values ≤ 10. The extent of the CPT data validates the thickness and consistencies of the compressible layers.

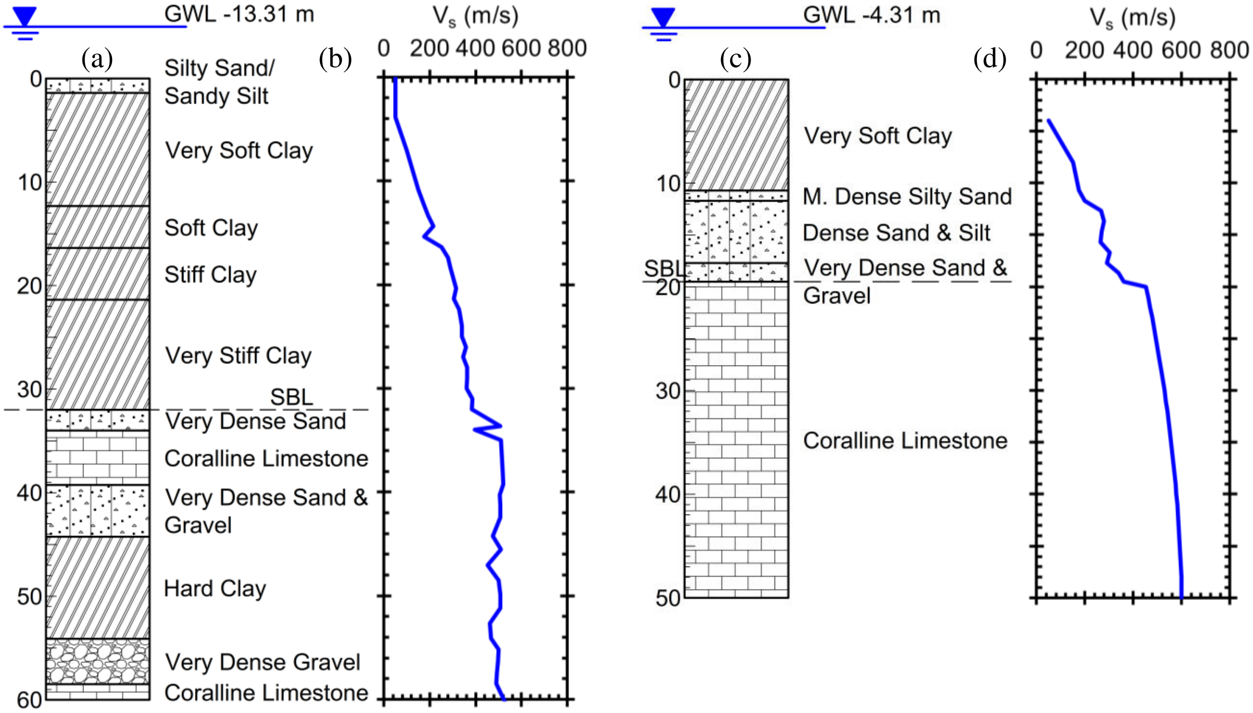

Figure 1: Idealized profiles from offshore site characterization data showing (a) stratification of a location 13.31 m below sea level and corresponding shear wave velocities in (b); (c) stratification of a location 4.31 m below sea level and corresponding shear wave velocities in (d).

Layers of very stiff to hard clays and silts, with lenses of dense to very dense sands and gravels found sporadically, underlie these compressible soil layers. Beneath these soil layers or friable soil-rock transition materials, a limestone-dominated rock formation showed up in the rock coring record until termination of the boreholes. Near the shore, the depth to the coralline limestone formation is around 15 to 20 m beneath the seabed.

Figure 1 also shows the location of the seismic base layer (SBL). This is the layer within the subsurface with a distinct/large contrast in stiffness between layers (i.e. stiffness impedance), with the bottom layer being relatively thick and having the larger stiffness. In most cases, the SBL is also the interface separating the soil cover and the rock formation. If the distinction is unclear, the contrast within the shear wave velocity profiles like Figure 1(b) and (d) can also serve as the basis for the SBL. From Figure 1, the SBL is generally located 20 to 30 m below the seabed. In site-specific hazard calculations where site effects are explicitly quantified, the SBL also serves as the boundary condition in site response simulations, where inputs are based on a reference rock condition—defined with a time-averaged shear wave velocity of all layers below the SBL.

3 SEISMIC HAZARD

The essential element of seismic hazard analysis is the integration of the information obtained from the seismic source models (SSM) (how or how often an earthquake will rupture) and ground motion models (how intense the earthquake is from the rupture). In this work, the site-specific seismic hazard calculation first dealt with a reference rock site (SBL) condition. The following subsections describe the seismic source characterization process and the calculation of the seismic hazard at the reference condition.

3.1 Seismic Sources

All reliable seismicity data sources shall be compiled first to get all possible earthquake events on record. Event records from the GEM global earthquake catalogue (Weatherill et al. 2016) and United States Geological Survey – National Earthquake Information Centre (USGS-NEIC) are utilized mainly in the overall catalogue for this work. In case of conflicts in location and magnitude, the former is prioritized over the latter. Historical (non-instrumental) records were also obtained from the work of Albini et al. (2014) to supplement the overall catalogue through further representation of moderate to strong earthquakes felt way before the advent of modern seismometry. However, as different record sources utilized various ways to reflect the earthquake size, all magnitude scales were homogenized into the moment magnitude scale using the relationships developed by Das et al. (2011). As probabilistic seismic hazard analysis normally works with Poissonian events, the aftershock sequences were filtered using the Gardner and Knopoff (1974) algorithm.

The main seismotectonic features in the central Philippines were delineated and constrained using the previous work by Galgana (2006) and by analyzing patterns of fault mechanism solutions (Ekström et al. 2012) in the region. In calibrating the recurrence relationships for each seismic source, the catalogue must be checked for completeness using the Stepp (1972) method to minimize artificial biases introduced by the lack of records prior to the mid-20th century. The calibration parameters for the recurrence relationships modeling the background seismic activity rates for each seismic source were then determined using the Weichert (1980) approach, which adopts maximum likelihood estimation despite the varying completeness levels in each sub-catalogue.

Fault sources included in the overall SSM represent active tectonic faults within the vicinity of the site. Geometric properties of the fault sources were obtained from Peñarubia et al. (2020), which provides an excellent compilation of all known active faults in the Philippines. The slip rate data reported by Styron and Pagani (2020) allowed the definition of alternative estimates to reflect the epistemic uncertainty both spatially and temporally.

Two alternative magnitude-frequency distributions were applied for the fault sources: the exponential and the characteristic earthquake model (Youngs and Coppersmith 1985). Meanwhile, subduction zone regions were also included in the overall SSM but later calculations implied that the effects of ruptures from these tectonic regions were insignificant compared to the ruptures from fault sources so they will not be discussed further in this paper.

3.2 Reference Hazard Estimate

With the SSM in place, ground motion models are required to gauge the intensity of earthquakes produced by each generated rupture. Modern ground motion models typically return a probability distribution, given by the median and standard deviation, of an intensity measure describing the ground motion. Even with this increased sophistication of modern ground motion models, these are still not completely unbiased. To account for epistemic uncertainty in ground motion prediction, four alternative models—ASK14 (Abrahamson et al. 2014), BSSA14 (Boore et al. 2014), CB14 (Campbell and Bozorgnia 2014), and CY14 (Chiou and Youngs 2014)—from the NGA-West 2 project were utilized in the seismic hazard calculations.

In DPWH-BSDS, different levels of ground motions—Level I and II—are associated with a combination of seismic performance levels, which are evaluated based on specified limits on structural response needed to attain satisfactory performance in view of safety, serviceability, and repairability. To facilitate the discussions herein, only the Level II ground motions will be the focus henceforth. The DPWH-BSDS defines the Level II ground motions as a hazard level with a 7% probability of exceedance (PoE) in 75 years or a 1,000-year return period (Fig. 2(a)). The Level II ground motions at this PoE are the ordinates of the uniform hazard spectrum (UHS) calculated using the OpenQuake Engine program (GEM Foundation 2021).

For comparison, the median (50th percentile) and 84th percentile deterministic spectra were calculated using the seismological parameters for a rupture scenario of the North Bohol Fault like the 2013 Bohol Earthquake (Rimando et al. 2019). The interesting match of the 84th deterministic spectrum with the full UHS indicates that the scenario at this level represents the hazard well at periods greater than 4 s. Nevertheless, the DPWH-BSDS stipulates that the seismic base envelope be taken to be not less than two-thirds of the UHS with 1,000-year return period within the range of 0.5 to 2.0 times the bridge fundamental period (shaded in green).

In Figure 2(b), five ground motion recordings were scaled to minimize the misfit in the period of interest. (The proper ground motion selection procedures will be discussed in Section 5.1.). Note also that the mean response spectra of the scaled base ground motions exceed the target spectrum (i.e. seismic base envelope in Figure 2(a)). Thus, the five scaled time histories are now ready to be applied as input for site response analysis.

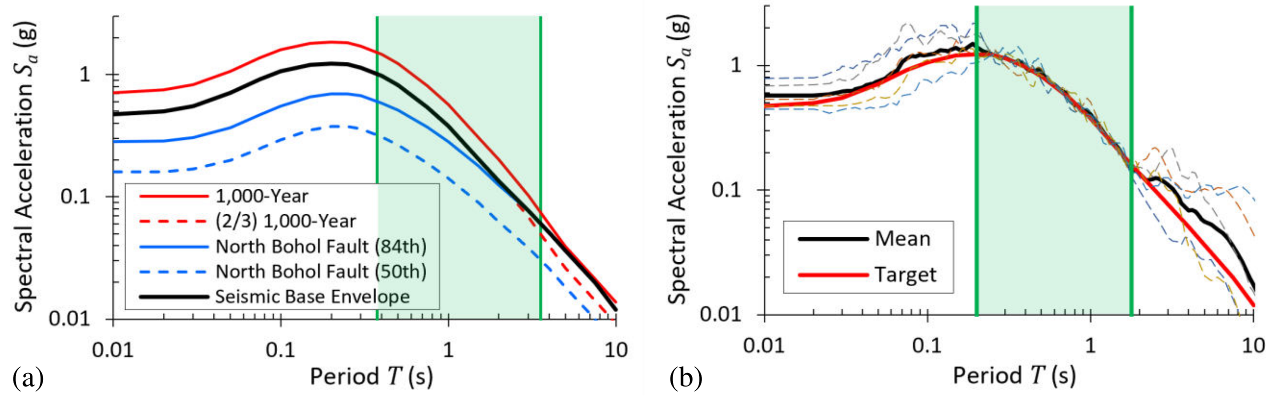

Figure 2: Plots of (a) development of 5%-damped SBL response spectra envelope for Level-II base motions; (b) scaled ground motions with their individual response spectra compatible with the envelope in (a).

4 VARIABILITY IN SITE RESPONSE

One-dimensional wave propagation analysis simulates the seismic wave transmission through the soil strata from the base layer, thereby leading to attenuation and amplification. Two methods are typically done for such analysis: equivalent-linear and nonlinear. Although both methods have their own merits, nonlinear analysis is more appropriate for very intense shaking, like a Level II ground motion, which is expected to induce significantly high shear strains. As such, only the results from the nonlinear site response analysis using the DEEPSOIL software (Hashash et al. 2020) will be presented in this section.

For the following discussions, the site response simulation results for Figures 1(a) and (b) will be in focus. As the characterization of geologic profiles, such as Figure 1(a) and (b), always exhibits variability regardless of measurement technique, the Toro (1995) geostatistical model was utilized to reflect the uncertainties in the computed surface response. For a given depth, the model assumes that shear wave velocity is log-normally distributed with a depth-dependent standard deviation and inter-layer correlation coefficient. In addition, it is also an option to generate realizations of modulus reduction and damping (MRD) curves in a Monte Carlo simulation to gauge the variability in a layer-specific manner.

Figure 3 shows the results of the site response simulations considering 30 randomized soil profiles and the best-estimate profile in Figure 1(b), subjected to the five pairs of scaled horizontal base motions. Spectral ratios, or seismic base-to-surface amplification factors, are presented in Figure 3(a) per realization (dashed grey lines) and for the best-estimate profile (solid blue line). As can be observed in Figure 3(a), attenuation or de-amplification of accelerations happen across the short-period intensities ($T < 0.83$ seconds) but for long-period accelerations, the intensities are amplified. On the other hand, the maximum amplification factor is 2.95 at 2.10 seconds. Note also that the mean spectral ratio (solid red line) for the 30 realizations closely resemble the best-estimate profile. This result indicates that the randomization set is large enough to represent the best-estimate profile with reasonable confidence.

The spectral ratios in Figure 3(a) were then smoothed and multiplied to the seismic base envelope in Figure 2(a). However, DPWH-BSDS also states that the spectral accelerations of the site-specific (smoothed) spectrum must not fall below two-thirds of the response spectrum constructed using the general procedure, within the period range of interest (Fig. 3(b)). The Level II ground motion envelope, representing the surface ground motion hazard, can then be obtained from the spectral ordinates satisfying these conditions. It is worth noting, however, that the compliance with DPWH-BSDS provisions on the minimum thresholds of site-specific hazard analysis results forced a localized jag or kink in the Level II envelope at around 3 to 5 seconds.

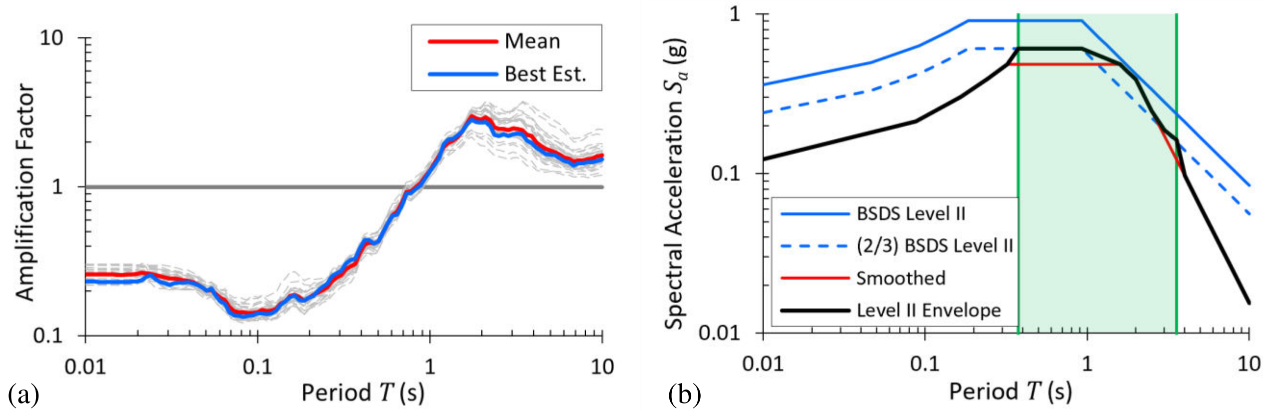

Figure 3: Plots of (a) spectral ratios of Level II motion (5% damping); (b) development of Level II Envelope.

5 TIME HISTORY DEVELOPMENT

5.1 Ground Motion Selection

According to DPWH-BSDS, nonlinear time-history analysis shall be performed with at least three pairs of appropriate time history records that match the target response spectrum characterizing the seismic hazard. If this ensemble of ground motions is used, design actions shall be taken as the maximum envelope of the responses calculated for all ground motions. The same sections or articles require that at least seven records be included in the ground motion suite for the average response to be considered.

Ground motions for evaluating structural performance shall be amplitude-compatible with the target response spectrum across a wide range of frequencies associated with the significant modes of vibration. Careful consideration is applied in selecting empirical seed (original, unscaled) ground motion time histories. Seismological features of the earthquake event and local site conditions at the recording station shall be consistent with the controlling earthquake scenario being considered (NIST, 2011). Ground motion recordings satisfying these criteria were downloaded from PEER NGA-West 2 database (PEER, 2012).

5.2 Ground Motion Modification

Spectral matching was done on SeismoMatch software by Seismosoft (2021). SeismoMatch performs matching using the wavelet algorithm of Al Atik and Abrahamson (2010), which is an update of the original algorithm proposed by Abrahamson (1992). This wavelet algorithm utilizes an improved tapered cosine adjustment function that prevents drift in the modified velocity and displacement time series without baseline correction. Figure 4(a) provides a sample comparison of a time history that is simply scaled versus a matched accelerogram that is response-spectrum compatible with the Level II envelope.

Figure 4(b) presents the matched 5%-damped maximum-direction (RotD100) response spectra (Boore 2010) of matched Level II horizontal ground motions, together with their respective suite average response spectra (solid black line) and target response spectra (solid red line). Consistent with ASCE 7-22 Section 16.2.3.3 requirements, amplitude compatibility of the mean matched spectra is essentially achieved (matches or is greater than 110% of the target) across the whole period range of interest (shaded in green). This type of check is not currently present in bridge seismic design standards but is carried out anyway to assess the effect of directionality on the matched ground motions.

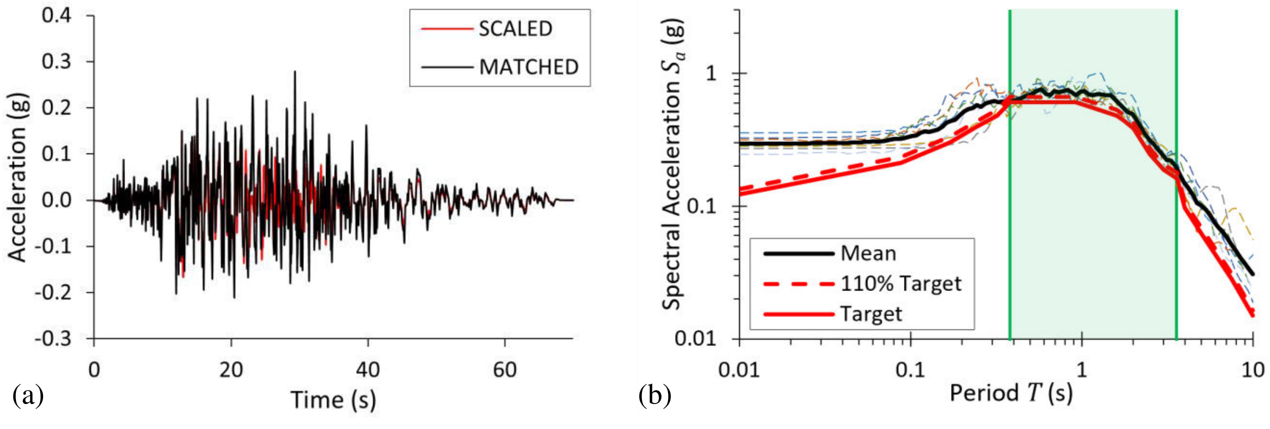

Figure 4: Plots of (a) spectral matching check using maximum-direction (RotD100) component of ground motions; (b) sample comparison between scaled and matched acceleration time histories.

6 CONCLUSIONS

This paper details the site-specific seismic hazard evaluation of a critical bridge infrastructure in Cebu, Philippines following local bridge seismic design provisions. A GI program revealed the relevant features of the bridge site in terms of their influence on the seismic hazard. The layer with a distinct contrast in the V_s profile (i.e. SBL) is generally located 20 to 30 m below the seabed. The seismic hazard calculation for the Level II ground motion first dealt with the reference rock site (SBL) condition. Then, nonlinear site response analysis made use of five base motions scaled to minimize misfit with the hazard at the SBL condition, along with 30 profile realizations to reflect the uncertainties in the computed surface response. A simple smoothing approach was applied to the simulation results for comparison with code-prescribed design spectra. Finally, the time-domain spectral matching procedure modified the seven pairs of horizontal-component recordings to be spectrum-compatible with the target Level II surface hazard.

Key issues can be highlighted in this work that need to be resolved to improve the practice in site-specific hazard studies. First, strict compliance with code provisions introduces jaggedness in design spectra envelopes. This may be acceptable when the spectral ordinates will be utilized directly, but when used as a target for developing time histories, the effect of the jagged target spectra on the acceptance of modified time-histories still needs to be further studied. Second, bridge design standards also need to incorporate more stringent requirements on time-history development, such as the maximum-direction (RotD100) checks in ASCE 7-22. Lastly, it may be time for design standards to recognize the benefits of non-ergodic hazard analysis—at least for site effects. Some difficulties may be encountered for data-poor regions and projects with limited number of performance level checks, as outlined by Luna et al. (2022), but the improved and (usually) reduced hazard may be extremely beneficial for the viability of large, critical projects.

7 REFERENCES

Abrahamson, N., Silva, W., and Kamai, R. (2014). Summary of the ASK14 ground motion relation for active crustal regions. *Earthquake Spectra*, 30(3), 1025-1055.

Al Atik, L. and Abrahamson, N. (2010). An Improved Method for Nonstationary Spectral Matching. *Earthquake Spectra*, 26(3), 601-617.

Albini, P., Musson, R. M. W., Rovida, A., Locati, M., Gomez Capera A. A., and Viganò D. (2014). The Global Earthquake History. *Earthquake Spectra*, 30(2), 607-624.

American Society of Civil Engineers (ASCE) (2022). *Minimum Design Loads and Associated Criteria for Buildings and Other Structures*. Reston, Virginia: American Society of Civil Engineers.

Boore, D. (2010). Orientation-independent, nongeometric-mean measures of seismic intensity from two horizontal components of motion. *Bull. Seismol. Soc. Am.*, 100(4), 1830-1835.

Boore, D., Stewart, J., Seyhan, E., and Atkinson, G. (2014). NGA-West2 equations for predicting PGA, PGV, and 5% damped PSA for shallow crustal earthquakes. *Earthquake Spectra*, 30(3), 1057-1685.

Campbell, K. and Bozorgnia, Y. (2014). NGA-West2 ground motion model for the average horizontal components of PGA, PGV, and 5% damped linear acceleration response spectra. *Earthquake Spectra*, 30(3), 1087-1114.

Chiou, B. and Youngs, R. (2014). Update of the Chiou and Youngs NGA model for the average horizontal component of peak ground motion and response spectra. *Earthquake Spectra*, 30(3), 1117-1153.

Das, R., Wason, H. and Sharma, M. (2011). Global regression relations for conversion of surface wave and body wave magnitudes to moment magnitude. *Natural Hazards*, 59(2), 801-810.

Department of Public Works and Highways (DPWH) and Japan International Cooperation Agency (JICA) (2013). LRFD Bridge Seismic Design Specifications (BSDS).

Department of Public Works and Highways (DPWH) (2019). BSDS Design Standard Guide Manual.

Ekström, G., Nettles, M., and Dziewoński, A. (2012). The global CMT project 2004-2010: Centroid-moment tensors for 13,017 earthquakes. *Physics of the Earth and Planetary Interiors*, 200-201, 1-9.

Galgana, G., Hamburger, M., McCaffrey, R., Corpuz, E., and Chen, Q. (2007). Analysis of crustal deformation in

Luzon, Philippines using geodetic observations and earthquake focal mechanisms. *Tectonophysics*, 432(1-4), 63-87.

Gardner, J. K. and Knopoff, L. (1974). Is the sequence of earthquakes in Southern California, with aftershocks removed, Poissonian? *Bull. Seismol. Soc. Am.*, 64(5), 1363–1367.

GEM Foundation. (2021). The OpenQuake Engine 3.12.1 User Manual.

Geotechnics Philippines, Inc. (GPI) (2022). Geotechnical Investigation works for Cebu-Mactan (4th bridge) Coastal Roads - Final Technical Report for Downhole Seismic Surveys.

Hashash, Y. M. A., Musgrove, M. I., Harmon, J. A., Ilhan, O., Xing, G., Numanoglu, O., Groholski, D. R., Phillips, C. A., and Park, D. (2020). DEEPSOIL 7.0. Urbana, Illinois, Board of Trustees of Univ. of Illinois at Urbana-Champaign.

Luna, R.A.C., Quebral, R.D., Selda, P.A.Y., Bernales, F.J.T., Sayson, S.B.R. (2022). Integrating Local Site Response Evaluations in Seismic Hazard Assessments. In: Wang, L., Zhang, JM., Wang, R. (eds) *Proc. of the 4th Intl. Conf. on Performance Based Design in Earthquake Geotechnical Engineering* (Beijing 2022). PBD-IV 2022. Geotechnical, Geological and Earthquake Engineering, vol 52. Springer, Cham.

National Institute of Standards and Technology (NIST) (2011). NIST GCR 11-917-15 Selecting and Scaling Earthquake Ground Motions for Performing Response-History Analyses.

Pacific Earthquake Engineering Research Center (PEER) (2012). PEER NGA-West2 Ground Motion Database. https://ngawest2.berkeley.edu.

Peñarubia, H. C., Johnson, K. L., Styron, R. H., Bacolcol, T. C., Sevilla, W. I. G., Perez, J. S., Bonita, J. D., Narag, I. C., Solidum, R. U., Pagani, M. M., and Allen, T. I. (2020). Probabilistic seismic hazard analysis model for the Philippines. *Earthquake Spectra*, 36(1_suppl), 44–68.

Rimando, J. M., Aurelio, M. A., Dianala, J. D. B., Taguibao, K. J. L., Agustin, K. M. C., Berador, A. E. G., and Vasquez, A. A. (2019). Coseismic ground rupture of the 15 October 2013 magnitude (M_W) 7.2 Bohol earthquake, Bohol Island, central Philippines. *Tectonics*, 38, 2558–2580.

Seismosoft. (2021). SeismoMatch - A computer program for spectrum matching of earthquake records.

Stepp, J. (1972). Analysis of Completeness of the Earthquake Sample in the Puget Sound Area and Its Effect on Statistical Estimates of Earthquake Hazard. *International Conference on Microzonification*, (1), 897-910.

Styron, R. and Pagani, M. (2020). The GEM Global Active Faults Database. *Earthquake Spectra* 36(SI), 160-180.

Toro, G. R. (1995). Probabilistic models of site velocity profiles for generic and site-specific ground-motion amplification studies. *Technical Report No. 779574*. Brookhaven National Laboratory, Upton, New York.

Unite, B. (2019). Build, Build, Build: A saga of big-ticket road projects to realize a dream travel across PH. *Republic of the Philippines – Public-Private Partnership Center*. Manila Bulletin, 2019.

Weatherill, G., Pagani, M., and Garcia, J. (2016). Exploring earthquake databases for the creation of magnitude-homogeneous catalogues: tools for application on a regional and global scale. *Geophys. J. Int.*, 206(3), 1652-1676.

Weichert, D. (1980). Estimation of earthquake recurrence parameters for unequal observation periods for different magnitudes. *Bull. Seismol. Soc. Am.*, 70(4), 1337-1346.

Youngs, R. and Coppersmith, K. (1985). Implications of Fault Slip Rates and Earthquake Recurrence Models to Probabilistic Seismic Hazard Estimates. *Bull. Seismol. Soc. Am.*, 75(4), 939-964.